Generalized Geometric Analysis of Right Circular Cylindrical Star Perforated and Tapered Grains

Andrea Ricciardi*
Agenzia Spaziale Italiana, Rome, Italy

This paper describes criteria and formulas adopted in developing a new computer program capable of evaluating the geometric evolution of a cylindrical star grain during its combustion. This computer program, named STAR, calculates the burning perimeter (or burning area), the wet perimeter, and port area as functions of burnt thickness for a cylindrical internally cone-shaped star grain. The star configuration is defined by seven geometric parameters. These parameters can be changed along the star grain in order to simulate different internal geometric shapes. The program does not utilize a lot of computer time and it is capable of analyzing a large number of star configurations for each run. This is very useful for a geometric optimization process of the star grain. The program output is organized in a file that can be directly used as an input file for the internal ballistic program.

Nomenclature

A_b = burning area
A_p = port area
N = number of star points
P_b = burning perimeter
P_w = wet perimeter
r_1 = fillet radius
r_2 = cusp radius
R = grain outside radius
W = web thickness in the cylindrical sector
W_c = variable web burnt
ϵ = angular fraction
ξ = star angle
η = star point semiangle

Introduction

THE computer program STAR was developed in order to evaluate the geometric evolution of a cylindrical star grain during its combustion. The star grain configuration considered is defined by the following seven independent geometric parameters: grain outside radius R, number of star points N, web thickness W, fillet radius r_1, cusp radius r_2, star angle ξ, and star point semiangle η. Sometimes instead of ξ, it is preferred to use a dimensionless parameter $\epsilon = \xi/(\pi/N)$ named angular fraction.[1-6]

The program is capable of considering two different configurations of the star point: 1) convex star point, and 2) concave star point, as shown in Fig. 1. The values of these parameters can be changed within large ranges, so that a very large number of star configurations can be drawn.

Based on the different geometric evolutions of the star during the web combustion, 16 configurations can be recognized: 8 with convex points and 8 with concave points. Analyzing the geometric evolutions of these 16 configurations, some web intervals were identified, named zones, in which burning perimeters, wet perimeters, and port areas can be evaluated, during the web consumption, by means of the same formulas.

As we can see in the next section, some of these zones can be found in more than one of the 16 configurations during their evolution.

Presented as Paper 89-2783 at the AIAA/ASME/ASEE/SAE 25th Joint Propulsion Conference, Monterery, CA, July 10-12, 1989; received Oct. 10, 1989; revision received April 9, 1990.

*Project Manager, Hypersonic Propulsion Program.

The total number of zones is 14; for each of them a program subroutine was dedicated to evaluate P_b, P_w, and A_p vs web. Clearly, these subroutines are called only by the configurations that need them.

The STAR program can run in two different ways:

1) Analyzing one star configuration at a time, evaluating P_b, P_w, and A_p as functions of burnt web. To speed up the geometric optimization process, many configurations can be analyzed for each run.

2) Analyzing cylindrical star grain with different possibilities of internal cone shaping and directly dividing the grain into longitudinal sectors in order to better prepare the input data for an internal ballistic computer program.

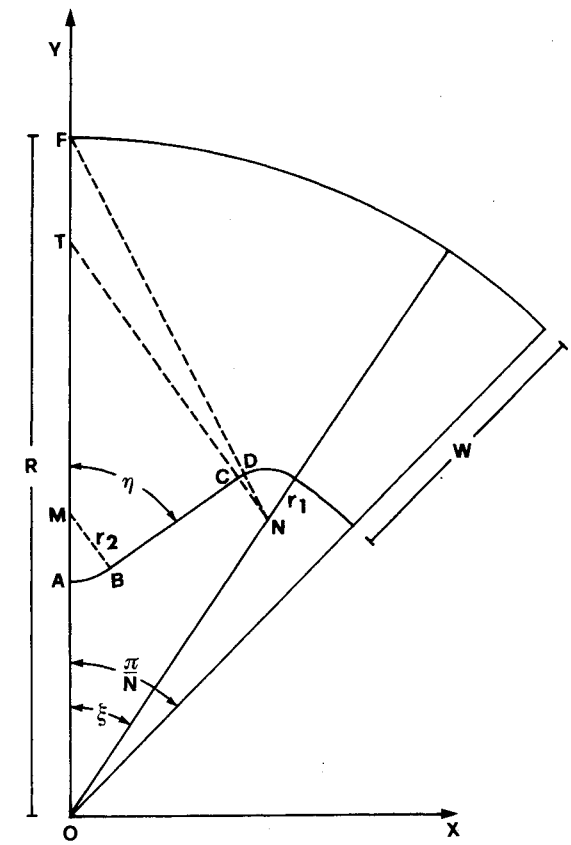

Fig. 1a Star configuration with convex point.

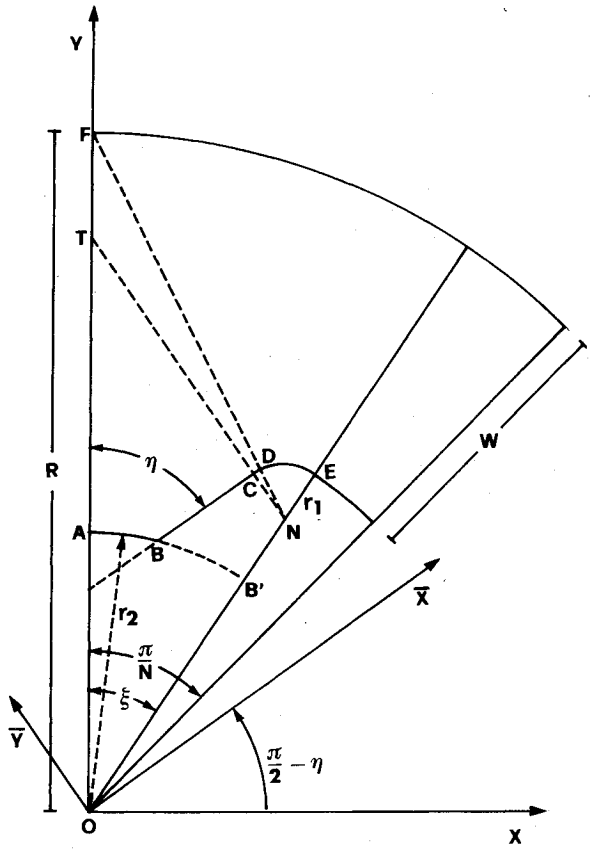

Fig. 1b Star configuration with concave point.

For each sector the program evaluates the burning area A_b, the wet perimeter P_w, and the port area A_p as functions of combustion web. The program is also able to evaluate the web fraction, volumetric loading fraction, and sliver fraction for each configuration.

Parameter Definition and Variability

The previously mentioned seven geometric parameters R, N, W, r_1, r_2, η, and ξ (or ϵ) univocally define the star configuration. However, for a complete geometric analysis the following additional parameters have to be considered:

$$ON = R - W - r_1$$

$$TC = ON\frac{\sin\xi}{\cos\eta} - r_1$$

$$OT = Y_t = ON(\cos\xi + \sin\xi\tan\eta)$$

$$\text{or} \quad OT = ON\cos\xi + (TC + r_1)\sin\eta$$

$$X_c = TC\cos\eta$$

$$Y_c = Y_t - TC\sin\eta$$

$$FN = \sqrt{(ON\sin\xi)^2 + (R - ON\cos\xi)^2}$$

$$FD = FN - r_1$$

and

$$FA = R - r_2$$

for the concave point.

To exclude the star configurations not possible from the geometric point of view or the ones not useful for ballistic purposes, the following range of variability of the main geometric parmeters are considered:

$$R > 0, \quad 0.5 \le \epsilon \le 1, \quad 3 \le N \le 20$$

$$0 < \eta < \pi/2, \quad 0 < W < R, \quad 0 < r_1 < (R - W)$$

and

$$0 \le r_2 \le TC$$

for the convex point, or

$$(Y_t - TC/\sin\eta) < r_2 < \sqrt{X_c^2 + Y_c^2}$$

for the concave point.

The program input are "filtered" by means of a subroutine, named FILTER, in order to avoid values of the parameters out of the ranges indicated above or that can cause interference between star points.

For the last problem, the following observations must be made. It was imposed that the star point should not exceed the circular sector delimited by the angle ξ. Also, if this condition eliminates some geometric configurations that are not particularly interesting from the ballistic point of view, it avoids interference between star points and simplifies the port area evaluation.

In case of a star with a convex point, the program imposes that the r_2 circumference should not have points in common with the line passing through O and N. The equations of the circumference and of the line are, respectively, $X^2 + (Y - Y_m)^2 = r_2^2$ and $Y = tX$, where $t = \tan(\pi/2 - \xi) = 1/\tan\xi$ and $Y_m = Y_t - (TC - r_2)/\sin\eta$. Substituting the second equation for the first one and imposing the condition of no interference ($\Delta < 0$, no solution for X), one has

$$Y_m - r_2\sqrt{1 + t^2} > 0 \tag{1}$$

In case of a star with a concave point, it is imposed that the ordinate of point B must be greater than the ordinate of point B′ (see Fig. 1b); therefore

$$Y_b \ge r_2\cos\xi \tag{2a}$$

or

$$Y_b - r_2\cos\xi \ge 0 \tag{2b}$$

Point B is calculated as the intersection between the circumference of r_2 radius and the line starting from C with angular coefficient $m = \tan(\pi/2 - \eta) = 1/\tan\eta$. Therefore, Y_b is given as

$$Y_b = \frac{-G\tan\eta + \sqrt{(G\tan\eta)^2 - (1 + \tan^2\eta)(G^2 - r_2^2)}}{1 + \tan^2\eta} \tag{3}$$

where

$$G = X_c - Y_c/m \tag{4}$$

The conditions given by Eqs. (1) and (2) assure no interference between the star points.

Geometric Configurations

In order to analyze all of the possible star configurations, with only the restrictions previously mentioned, a detailed geometric analysis was performed. The star configurations are divided into two groups: stars with convex points (8 configurations) and stars with concave points (8 configurations). Each star configuration can be divided into web zones in which the relationships for the evaluation of the geometric variables (P_b, P_w, A_p) are constant.

In the following, all of the configurations analyzed and the relative intervals of the geometric parameters are reported. To avoid a paper that is too long, only the figures of the configurations showing new zones are reported.

The star configurations with convex points are:

Configuration 1: ($r_2 < TC$) and ($TC < W$) (see Fig. 2):

$0 \le W_c < r_2$,	zone 1
$r_2 \le W_c < TC$,	zone 2
$TC \le W_c < W$,	zone 3
$W < W_c \le FD$,	zone 4

Zone 3 disappears if $TC = W$

Configuration 2: ($r_2 < W$) and ($W < TC < FD$) (see Fig. 3):

$0 \le W_c < r_2$,	zone 1
$r_2 \le W_c < W$,	zone 2
$W \le W_c < TC$,	zone 5
$TC \le W_c \le FD$,	zone 4

Zone 5 disappears if $TC = W$
Zone 4 disappears if $TC = FD$

Configuration 3: ($r_2 < W$) and ($TC > CP_o$) (see Fig. 4):

$0 \le W_c < r_2$,	zone 1
$r_2 \le W_c < W$,	zone 2
$W \le W_c < CQ_o$,	zone 5
$CQ_o \le W_c \le CP_o$,	zone 6

Zone 2 disappears if $r_2 = W$

Configuration 4: ($r_2 = W$) and ($W < TC < FD$):

$0 \le W_c < W$,	zone 1
$W \le W_c < TC$,	zone 5
$TC \le W_c \le FD$,	zone 4

Zone 4 disappears if $TC = FD$

Configuration 5: ($W < r_2 < TC$) and ($W < TC < FD$) (see Fig. 5):

$0 \le W_c < W$,	zone 1
$W \le W_c < r_2$,	zone 7
$r_2 \le W_c < TC$,	zone 5
$TC \le W_c \le FD$,	zone 4

Zone 4 disappears if $TC = FD$

Configuration 6: ($W < r_2 < CQ_o$) and ($TC > CP_o$):

$0 \le W_c < W$,	zone 1
$W \le W_c < r_2$,	zone 7
$r_2 \le W_c < CQ_o$,	zone 5
$CQ_o \le W_c \le CP_o$,	zone 6

Zone 5 disappears if $r_2 = CQ_o$

Configuration 7: ($CQ_o < r_2 < CP_o$) and ($TC > CP_o$):

$0 \le W_c < W$,	zone 1
$W \le W_c < CQ_o$,	zone 7

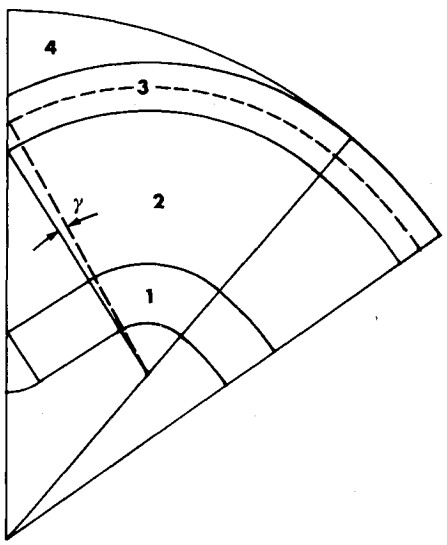

Fig. 2 Star configuration 1, convex point.

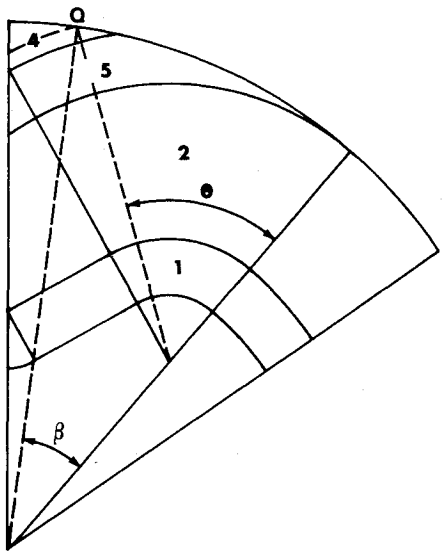

Fig. 3 Star configuration 2, convex point.

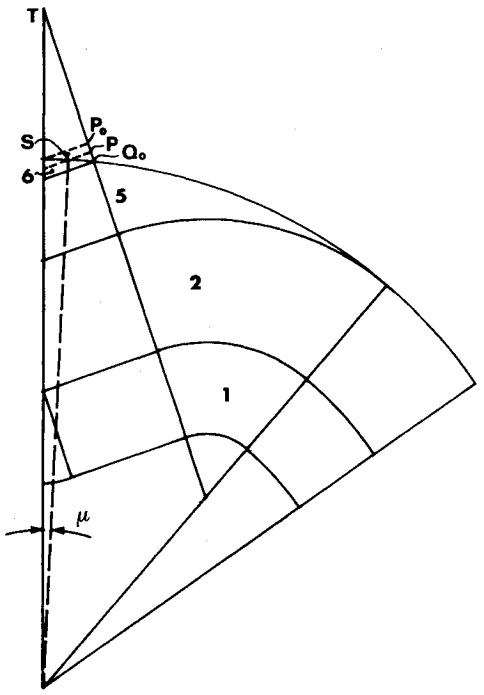

Fig. 4 Star configuration 3, convex point.

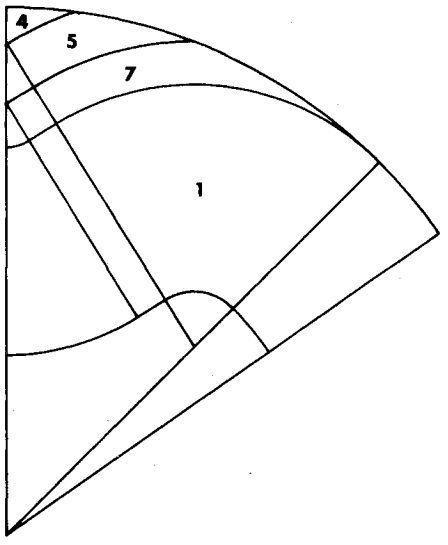

Fig. 5 Star configuration 5, convex point.

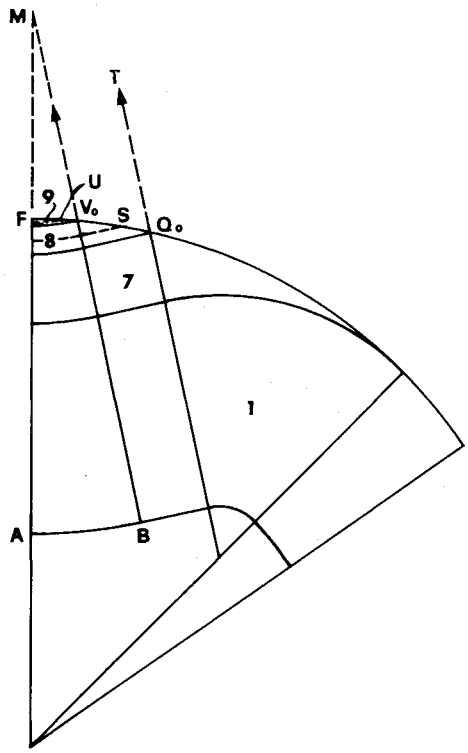

Fig. 6 Star configuration 8, convex point.

$$CQ_o \le W_c < r_2, \quad \text{zone 8}$$
$$r_2 \le W_c \le CP_o, \quad \text{zone 6}$$

Zone 6 disappears if $r_2 = CP_o$

Configuration 8: $(r_2 > CP_o)$ and $(TC > CP_o)$ (see Fig. 6):

$$0 \le W_c < W, \quad \text{zone 1}$$
$$W \le W_c < CQ_o, \quad \text{zone 7}$$
$$CQ_o \le W_c < BV_o, \quad \text{zone 8}$$
$$BV_o \le W_c \le AF, \quad \text{zone 9}$$

Before showing the star configurations with concave points, some geometric considerations must be made. First of all, it is necessary to know the curve obtained with the intersection points between the rectilinear combustion front BC and the circular one AB (Fig. 1b) during combustion. If this curve intersects the segment TC, it means the rectilinear front disappears and the two circular combustion fronts AB and CE come in contact, therefore obtaining another intersection curve during combustion. The equation of the first curve (intersection between AB and BC) can be obtained more easily by considering new reference axes $\bar{X}$, $\bar{Y}$ obtained by rotating the main axes X, Y of an angle $(\pi/2-\eta)$ counterclockwise (Fig. 1b).

In this new system, the equation of this curve is

$$\bar{X}^2 - 2(r_2 - \bar{Y}_b)\bar{Y} - (r_2 - \bar{Y}_b)^2 = 0 \tag{5}$$

where $\bar{Y}_b$ is the ordinate of point B in the new system. Clearly, in this case only the positive value of $\bar{X}$ is of interest. Now it is possible to know the intersection point I between this curve and the line passing through T and C; the ordinate of this point is

$$\bar{Y}_i = \frac{\bar{X}_t^2 - (r_2 - \bar{Y}_b)^2}{2(r_2 - \bar{Y}_b)} \tag{6}$$

If $\bar{Y}_i$ is greater than $\bar{Y}_t$, it means that there is no intersection between this curve and the segment TC, but necessarily there will be an intersection between the curve and the main axis Y. The abscissa value of intersection point H (Fig. 7) is evaluated by considering the system as constituted of Eq. (5) and the

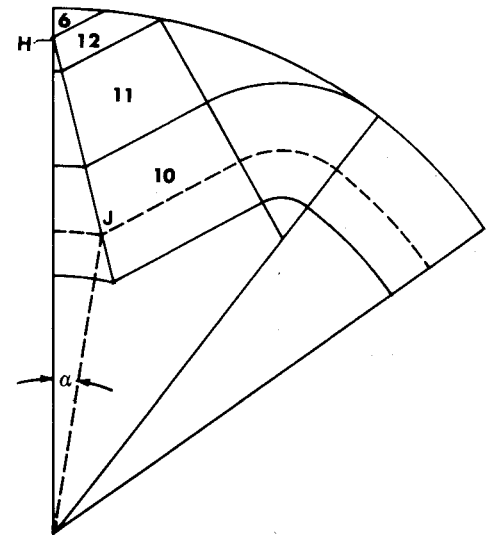

Fig. 7 Star configuration 9, concave point.

equation of the Y axis in the new system ($\bar{Y} = \tan\eta\,\bar{X}$). The abscissa is

$$\bar{X}_h = (r_2 - \bar{Y}_b)(\tan\eta + \sqrt{1 + \tan^2\eta}) \tag{7}$$

and the combustion web at which this intersection occurs is

$$W_{c1} = \frac{\bar{X}_h}{\sin(\pi/2 - \eta)} - r_2 \tag{8}$$

On the contrary, if there is intersection between the curve and segment TC (it means $\bar{Y}_i < \bar{Y}_t$), then the combustion web at which this intersection occurs is

$$W_{c2} = \bar{Y}_i - \bar{Y}_b \tag{9}$$

In this second case, after web W_{c2}, the combustion front is constituted of two arcs of circumferences which cross each other. The curve created by these intersection points during combustion can be determined more easily by considering a new system of reference axes X', Y', obtained rotating the main axis X, Y of an angle ξ in clockwise direction. The equation of this curve is

$$X'^2 + (1 - A^2)Y'^2 - 2(r_2 - B)AY' - (r_2 - B)^2 = 0$$

where

$$A = ON/(r_2 - r_1)$$

and

$$B = \frac{(r_2^2 - r_1^2) + ON^2}{2(r_2 - r_1)}$$

This curve intersects axis Y (in the new system $Y' = -X'/\tan\xi$) at point Ω (Fig. 8); the abscissa X'_Ω is

$$X'_\Omega = \left(-D - \sqrt{D^2 + CE}\right)/C$$

where

$$C = 1 + (1 - A^2)\cot^2\xi$$
$$D = A(r_2 - B)\cot\xi$$
$$E = (r_2 - B)^2$$

The combustion web at which this intersection occurs is

$$W_{c3} = -X'_\Omega/\sin\xi - r_2 \tag{10}$$

The values of W_{c1}, W_{c2}, and W_{c3} are useful to define star configurations and web zones.

The star configurations with concave points are:

Configuration 9: $(TC > CP_o)$ and $(CQ_o < W_{c1} < CP_o)$ (see Fig. 7):

$0 \le W_c < W$, zone 10
$W \le W_c < CQ_o$, zone 11
$CQ_o \le W_c < W_{c1}$, zone 12
$W_{c1} \le W_c \le CP_o$, zone 6

Zone 6 disappears if $W_{c1} = CP_o$

Configuration 10: $(TC > CP_o)$ and $(W_{c1} > R - r_2)$:

$0 \le W_c < W$, zone 10
$W \le W_c < CQ_o$, zone 11
$CQ_o \le W_c \le FA$, zone 12

Configuration 11: $(W_{c2} < W_{c3})$ and $(W_{c3} < W)$ (see Fig. 8):

$0 \le W_c < W_{c2}$, zone 10
$W_{c2} \le W_c < W_{c3}$, zone 13
$W_{c3} \le W_c < W$, zone 3
$W \le W_c \le FD$, zone 4

Zone 3 disappears if $W_{c3} = W$

Configuration 12: $(W_{c2} < W)$ and $(W < W_{c3} < R - r_2)$ (see Fig. 9):

$0 \le W_c < W_{c2}$, zone 10
$W_{c2} \le W_c < W$, zone 13
$W \le W_c < W_{c3}$, zone 14
$W_{c3} < W_c \le R - r_2$, zone 4

Zone 4 disappears if $W_{c3} = R - r_2$
Zone 13 disappears if $W_{c2} = W$

Configuration 13: $(W_{c2} < W)$ and $(W_{c3} > R - r_2)$:

$0 \le W_c < W_{c2}$, zone 10
$W_{c2} \le W_c < W$, zone 13
$W \le W_c \le FA$, zone 14

Zone 13 disappears if $W_{c2} = W$

Configuration 14: $(W < W_{c2})$ and $(W_{c2} < W_{c3} < R - r_2)$:

$0 \le W_c < W$, zone 10
$W \le W_c < W_{c2}$, zone 11
$W_{c2} \le W_c < W_{c3}$, zone 14
$W_{c3} \le W_c \le FD$, zone 4

Zone 4 disappears if $W_{c3} = R - r_2$

Configuration 15: $(W < W_{c2} < R - r_2)$ and $(W_{c3} > R - r_2)$:

$0 \le W_c < W$, zone 10
$W \le W_c < W_{c2}$, zone 11
$W_{c2} \le W_c \le FA$, zone 14

Zone 14 disappears if $W_{c2} = R - r_2$:

Configuration 16: $(W_{c2} > R - r_2)$:

$0 \le W_c < W$, zone 10
$W \le W_c < CQ_o$, zone 11
$CQ_o \le W_c \le R - r_2$, zone 12

The relationships for the evaluation of P_b, P_w, and A_p as functions of the burnt web thickness W_c are reported in the next section.

Geometric Relationships

All of the geometric relationships used to calculate burning perimeter P_b, wet perimeter P_w, and port area A_p as functions of burned perimeter W_c for the 14 zones previously shown are reported in this section. No simplification of the relationships are performed, in order to distinguish more simply each contribution to the perimeters and port area.

Zone 1:

$$P_b = P_w = (R - W + W_c)(\pi/N - \xi) + (r_1 + W_c)(\pi/2 - \eta + \xi) + \frac{(TC - r_2)}{\tan\eta} + (r_2 - W_c)(\pi/2 - \eta)$$

$$A_p = \frac{(R - W + W_c)^2}{2}(\pi/N - \xi) + \frac{(r_1 + W_c)^2}{2}(\pi/2 - \eta + \xi) + \frac{ON\,Y_t}{2}\sin\xi - \frac{(TC - W_c)^2}{2\tan\eta} + \frac{(r_2 - W_c)^2}{2\tan\eta} - \frac{(r_2 - W_c)^2}{2}(\pi/2 - \eta)$$

Zone 2:

$$P_b = P_w = (R - W + W_c)(\pi/N - \xi) + (r_1 + W_c)(\pi/2 - \eta + \xi) + \frac{(TC - W_c)}{\tan\eta}$$

$$A_p = \frac{(R - W + W_c)^2}{2}(\pi/N - \xi) + \frac{(r_1 + W_c)^2}{2}(\pi/2 - \eta + \xi) + \frac{ON\,Y_t}{2}\sin\xi - \frac{(TC - W_c)^2}{2\tan\eta}$$

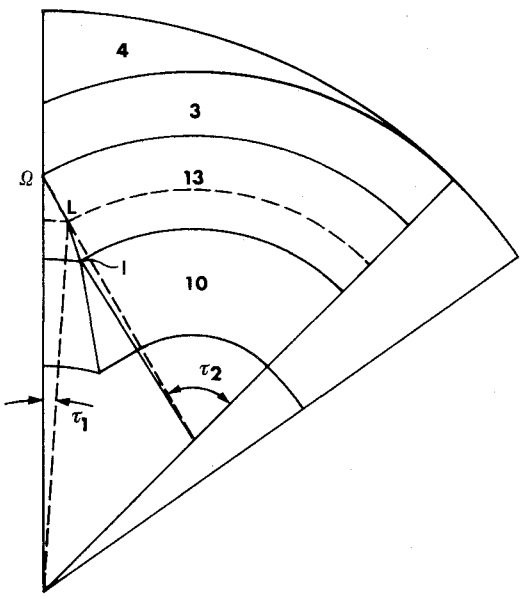

Fig. 8 Star configuration 11, concave point.

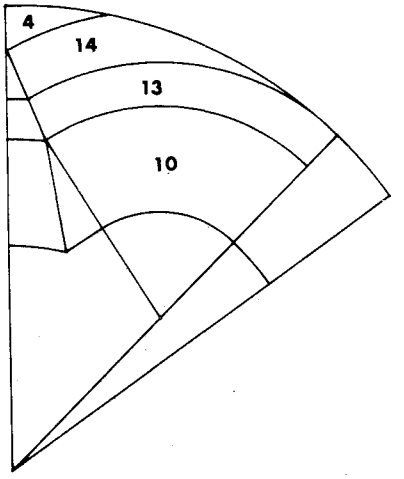

Fig. 9 Star configuration 12, concave point.

Zone 3:

$$P_b = P_w = (R - W - W_c)(\pi/N - \xi) + (r_1 + W_c)(\pi/2 - \eta + \xi - \gamma)$$

where

$$\gamma = \arccos\left(\frac{TC + r_1}{r_1 + W_c}\cos\eta\right) - \eta, \qquad 0 < (\gamma + \eta) < \pi$$

$$A_p = \frac{(R - W + W_c)^2}{2}(\pi/N - \xi) + \frac{(r_1 + W_c)^2}{2}(\pi/2 - \eta + \xi - \gamma) + \frac{ON}{2}(r_1 + W_c)\sin(\pi/2 + \eta - \xi + \gamma)$$

Zone 4:

$$P_b = (r_1 + W_c)(\pi/2 - \eta + \xi - \gamma - \theta)$$

$$P_w = P_b + R(\pi/N - \xi + \beta)$$

$$A_p = \frac{R^2}{2}(\pi/N - \xi + \beta) - \frac{R}{2}ON\sin\beta + \frac{(r_1 + W_c)^2}{2}(\pi/2 - \eta + \xi - \gamma - \theta) + \frac{(r_1 + W_c)}{2}ON\sin(\pi/2 + \eta - \xi + \gamma)$$

where γ is the angle previously defined, θ and β are the angles shown in Fig. 3 and evaluated by means of

$$\beta = \xi - \arccos\frac{Y_q}{R}, \qquad 0 < (\xi - \beta) < \pi$$

$$\theta = \arcsin\left(\frac{R}{r_1 + W_c}\sin\beta\right)$$

where Y_q is the ordinate of the intersection point Q calculated by means of

$$Y_q = \left\{A\left(\frac{Y_n}{X_n}\right) + \sqrt{A^2\left(\frac{Y_n}{X_n}\right)^2 - \left[1 + \left(\frac{Y_n}{X_n}\right)^2\right](A^2 - R^2)}\right\} \times \left[1 + \left(\frac{Y_n}{X_n}\right)^2\right]^{-1}$$

and

$$A = \left[R^2 + X_n^2 + Y_n^2 - (r_1 + W_c)^2\right]/(2X_n)$$

Zone 5:

$$P_b = (r_1 + W_c)(\pi/2 - \eta + \xi - \theta) + \frac{TC - W_c}{\tan\eta}$$

$$P_w = P_c + R(\pi/N - \xi + \beta)$$

$$A_p = \frac{R^2}{2}(\pi/N - \xi + \beta) - \frac{R}{2}ON\sin\beta + \frac{(r_1 + W_c)^2}{2}(\pi/2 - \eta + \xi - \theta) + \frac{ON\,Y_t}{2}\sin\xi - \frac{(TC - W_c)^2}{2\tan\eta}$$

where β and θ are the previously defined angles.

Zone 6:

$$P_b = \frac{X_s}{\sin\eta}$$

$$P_w = P_b + R(\pi/N - \mu)$$

where

$$\mu = \arcsin(X_s/R)$$

$$A_p = \frac{R^2}{2}(\pi/N - \mu) + \frac{R}{2}\left(Y_t - \frac{TC - W_c}{\sin\eta}\right)\sin\mu$$

where

$$X_s = \left\{-n(Y_p - nX_p) + \sqrt{n^2(Y_p - nX_p)^2 - (1 + n^2)\left[(Y_p - nX_p)^2 - R^2\right]}\right\}/(1 + n^2)$$

$$n = \tan(\pi/2 - \eta), \quad X_p = (TC - W_c)\cos\eta$$

$$Y_p = Y_t - (TC - W_c)\sin\eta$$

Zone 7:

$$P_b = (r_2 - W_c)(\pi/2 - \eta) + \frac{(TC - r_2)}{\tan\eta} + (r_1 + W_c)(\pi/2 - \eta + \xi - \theta)$$

$$P_w = P_b + R(\pi/N - \xi + \beta)$$

$$A_p = \frac{R^2}{2}(\pi/N - \xi + \beta) - \frac{R}{2}ON\sin\beta + \frac{(r_1 + W_c)^2}{2}(\pi/2 - \eta + \xi - \theta) + \frac{(TC + r_1)}{2}ON\sin(\pi/2 + \eta - \xi) - \frac{(TC - W_c)^2}{2\tan\eta} + \frac{(r_2 - W_c)^2}{2\tan\eta} - \frac{(r_2 - W_c)^2}{2}(\pi/2 - \eta)$$

where the angles θ and β are reported in zone 4.

Zone 8:

$$P_b = \frac{X_s}{\sin\eta} - \frac{(r_2 - W_c)}{\tan\eta} + (r_2 - W_c)(\pi/2 - \eta)$$

$$P_w = P_b + R(\pi/N - \mu)$$

$$A_p = \frac{R^2}{2}(\pi/N - \mu) + \frac{R}{2}\left[Y_t - \frac{(TC - W_c)}{\sin\eta}\right]\sin\mu + \frac{(r_2 - W_c)^2}{2\tan\eta} - \frac{(r_2 - W_c)^2}{2}(\pi/2 - \eta)$$

where X_s and μ are defined in zone 6.

Zone 9:

$$P_b = (r_2 - W_c)\sigma$$

$$P_w = P_b + R(\pi/N - \delta)$$

$$A_p = \frac{R^2}{2}(\pi/N - \delta) + \frac{Y_m R}{2}\sin\delta - \frac{(r_2 - W_c)^2}{2}\sigma$$

where δ and σ are the angles shown in Fig. 6 and evaluated by means of $\delta = \arccos(Y_u/R)$

and

$$\sigma = \arccos\left(\frac{Y_m - Y_u}{r_2 - W_c}\right)$$

The ordinates of point U are

$$Y_u = \frac{R^2 + Y_m^2 - (r_2 - W_c)^2}{2Y_m}, \qquad X_u = \sqrt{(R^2 - Y_u)^2}$$

Zone 10:

$$P_b = (r_2 + W_c)\alpha + \frac{TC - W_c}{\tan\eta} - \frac{X_j}{\sin\eta} + (r_1 + W_c)(\pi/2 - \eta + \xi) + (R - W + W_c)(\pi/N - \xi)$$

$$P_w = P_b$$

$$A_p = \frac{(R - W + W_c)^2}{2}(\pi/N - \xi) + \frac{(r_1 + W_p)^2}{2}(\pi/2 - \eta + \xi) + \frac{ON}{2}(TC + r_1)\cos(\xi - \eta) - \frac{(TC - W_c)^2}{2\tan\eta} + \frac{(r_2 + W_c)^2}{2}\alpha - \frac{(r_2 + W_c)}{2}\frac{X_j}{\sin\eta}\sin(\eta - \alpha)$$

where the angle α and the point J are shown in Fig. 7.

$$\alpha = \arcsin\left(\frac{X_j}{r_2 + W_c}\right)$$

$$X_j = \frac{-K\cot\eta + \sqrt{(K\cot\eta)^2 - (1 + \cot\eta)\left[K^2 - (r_2 + W_c)^2\right]}}{(1 + \cot^2\eta)}$$

$$K = Y_t - (TC - W_c)/\sin\eta$$

Zone 11:

$$P_b = (r_2 + W_c)\alpha + \frac{(TC - W_c)}{\tan\eta} - \frac{X_j}{\sin\eta} + (r_1 + W_c)(\pi/2 - \eta + \xi - \theta)$$

$$P_w = P_b + R(\pi/N - \xi + \beta)$$

$$A_p = \frac{R^2}{2}(\pi/N - \xi + \beta) - \frac{R\,ON}{2}\sin\beta + \frac{(r_1 + W_c)^2}{2}(\pi/2 - \eta + \xi - \theta) + \frac{Y_t ON}{2}\sin\xi - \frac{(TC - W_c)^2}{2\tan\eta} + \frac{(r_2 + W_c)^2}{2}\alpha - \left(Y_t - \frac{TC - W_c}{\sin\eta}\right)\frac{(r_2 + W_c)}{2}\sin\alpha$$

where β and θ are defined in zone 4 and α and X_j are defined in zone 10.

Zone 12:

$$P_b = \frac{X_s}{\sin\eta} - \frac{X_j}{\sin\eta} + (r_2 + W_c)\alpha$$

$$P_w = P_b + R(\pi/N - \mu)$$

$$A_p = \frac{R^2}{2}(\pi/N - \mu) + \frac{R}{2}(r_2 + W_c)\sin(\mu - \alpha) + \frac{(r_2 + W_c)^2}{2}\alpha$$

where X_s and μ are defined in zone 6 and X_j and α are defined in zone 10.

Zone 13:

$$P_b = (r_2 + W_c)\tau_1 + (r_1 + W_c)\tau_2 + (R - W + W_c)(\pi/N - \xi)$$

$$P_w = P_b$$

$$A_p = \frac{(r_2 + W_c)^2}{2}\tau_1 + \frac{ON}{2}(r_2 + W_c)\sin(\xi - \tau 1) + \frac{(r_1 + W_c)^2}{2}\tau_2 + \frac{(R - W + W_c)}{2}(\pi/N - \xi)$$

where the point L and the angles τ_1, τ_2 are shown in Fig. 8 and evaluated by means of

$$\tau_1 = \arccos\left(\frac{Y_1}{r_2 + W_c}\right), \quad \tau_2 = \xi + \tau, \quad \tau = \arccos\left(\frac{Y_1 - Y_n}{r_1 + W_c}\right)$$

$$Y_1 = \left\{C(Y_n/X_n) + \sqrt{\left[C(Y_n/X_n)\right]^2 - \left[1 + (Y_n/X_n)^2\right]\left[C^2 - (r_2 + W_c)^2\right]}\right\} \times \left[1 + (Y_n/X_n)^2\right]^{-1}$$

and

$$C = \left[(r_2 + W_c)^2 - (r_1 + W_c)^2 + X_n^2 + Y_n^2\right]/(2X_n)$$

Zone 14:

$$P_b = (r_2 + W_c)\tau_1 + (r_1 + W_c)(\tau_2 - \theta)$$

$$P_w = P_b + R(\pi/N - \xi + \beta)$$

$$A_p = \frac{R^2}{2}(\pi/N - \xi + \beta) - \frac{R}{2}ON\sin\beta + \frac{(r_2 + W_c)^2}{2}\tau_1 + \frac{(r_2 + W_c)}{2}ON\sin(\xi - \tau_1) + \frac{(r_1 + W_c)^2}{2}(\tau_2 - \theta)$$

where θ and β are defined in zone 4 and τ_1 and τ_2 are defined in zone 13.

Program Structure

The program is structured with the following subroutines:

FILTER: This subroutine "filters" the geometric input parameters in order to avoid geometrically impossible star configurations or values of parameters outside the ranges previously mentioned.

CONVEX: This subroutine can analyze only the eight star configurations with convex points.

CONCAVE: This subroutine can analyze the eight star configurations with concave points.

These last two subroutines are structured following the same logical organization of the paragraph: geometric configurations. Namely, based on the values of the geometric parameters, they call only the subroutines of the zones of interest.

ZONE 1 ··· ZONE 14: These are 14 subroutines capable of evaluating P_b, P_w, and A_p vs the variable web burnt W_c. The relationships adopted in these subroutines are the ones reported in the previous section.

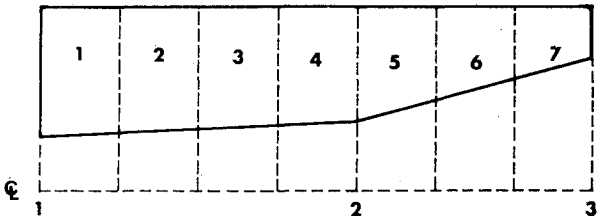

Fig. 10 Cylindrical star grain with two different tapered zones.

As mentioned in the Introduction, the program can run in two different ways. In the first way, the program analyzes exactly one star configuration at a time (or more, but separately); therefore the program needs only the seven geometrical parameters of the star and the delta-web ΔW_c for which P_b, P_w, and A_p have to be evaluated. Clearly, whatever ΔW_c may be, the program always gives the values of P_b, P_w, and A_p for the values of W_c where a transition from one zone to another occurs; for example for $W_c = W$ or $W_c = TC$, etc. In the second case, the input is the grain length and the values of the seven geometrical parameters along the grain. For example, if the grain has a constant star perforation, only one set of the seven geometrical parameters is necessary. If the grain is internally tapered, it is necessary to give the constant grain outside radius R and two sets of the remaining six parameters only at the beginning and at the end of the tapered zone.

In the same way, if the grain has different tapered zones (two in Fig. 10), the six parameters must be given to the program only at the stations along the grain axis where the cone-shape changes (at stations 1, 2, and 3 of Fig. 10).

The number of longitudinal sectors in which the star grain should be subdivided must be specified in order to prepare the output in such a way as to be directly used as input of the internal ballistic program (in Fig. 10 the grain is subdivided into seven longitudinal sectors). For each longitudinal sector the program calculates the burning area A_b, as product of the P_b (evaluated in the middle of the sector) and the sector length, the wet perimeter, and port area at each delta increase of the web. Clearly, if the grain is internally tapered, the values of P_b, P_w, and A_p in the middle of each sector are evaluated considering a star with the six parameters obtained by means of linear interpolation between the values of the sector extremities. In this case, the evaluated values are approximated, but according to our experience, if the cone semiangle is less than 10–15 deg the error on A_b is less than 1–2%. However, from the geometric point of view, it is useful to increase the number of longitudinal sectors in the tapered zone in order to reduce the error on the evaluated parameters, especially concerning the total combustion web and the total propellant weight.

Conclusions

The described star program is able to evaluate exactly the geometrical evolution of a cylindric star grain. If there is a variation of the seven geometrical parameters along the grain axis, the solutions have to be considered as approximated. But, if the cone semiangle is less than 10–15 deg, the error in A_b is less than 1–2%.

The program output is organized in a file that can be directly used for the subsequent internal ballistic analysis. The program is provided with a postprocessor capable of drawing, by means of a plotter, the star configuration vs W_c and the diagrams of P_b (or the burning surface), P_w, and A_p as functions of W_c. It is also capable of evaluating the web fraction, the volumetric loading fraction, and sliver fraction. Since the program can analyze a large number of star configurations in little time, it is particularly suited for geometrical optimization of the grain. For example, an optimization process that involves the calculation of 100 configurations or, equivalently, a star grain divided in 100 longitudinal sectors, will take 10 or 30 min of CPU time (IBM 3090) depending on the selected delta web. Frequently, in engineering practice it is not fundamental to have a neutral burning star, but is can be necessary to have a star with a small sliver fraction (for example, the booster of Ariane 3), or a large initial burning surface (as for some micro-rocket igniters), or a star grain with a high volumetric loading fraction (as for space motor), and so on.

These requirements can be satisfied only by means of an optimization process that can be speedy and efficient only by using a computer program.

For the program validation, 15 star configurations were drawn on a very large scale. The values of P_b, P_w, and A_p vs W_c directly measured on the drawings are in perfect accordance with the calculated values.

References

[1]Barrere, M., Jaumotte, A., Venbeke, B. F., and Vandenkerckhove, J., *Rocket Propulsion*, Elsevier Publishing Co., Amsterdam, 1960, Sec. 6.2.

[2]Stone, M. W., "A Practical Mathematical Approach to Grain Design," *Jet Propulsion*, Vol. 28, April 1958, pp. 236–244.

[3]Williams, F. A., Barrere, M., and Haung, N. C., *Fundamental Aspects of Solid-Propellant Rockets*, Technivision Services, Slough, England, 1969.

[4]Krishnan, S., "Design of Neutral Burning Star Grains," *Journal of Spacecraft*, Vol. 12, No. 1, 1975, pp. 60–62.

[5]Brooks, W. T., "An Exact Practical Analysis of the Ballistic Star Configuration," *Proceedings of 1979 JANNAF Propulsion Meeting*, CPIA Pub. 300, Vol. II, May 1979, pp. 343–361.

[6]Brooks, W. T., "Ballistic Optimization of the Star Grain Configuration," *Journal of Spacecraft*, Vol. 19, No. 1, 1982, pp. 54–59.